Mechanical fatigue properties of self-supported nano-layered composites

Yun-Che Wang[†]

[†]Assistant Professor
Department of Civil Engineering
National Cheng Kung University
Tainan, Taiwan

Abstract

This article is intended to provide a review regarding the recent development of nano-layered composites for their superior mechanical properties, such as high yield strength, ductility, and fatigue endurance. A particular focus is on the fatigue properties of the self-supported nano-multilayers. The nano-scale multilayers of interest are magnetron sputtered, copper-based systems, e.g. Cu/Nb, with alternating material layers and the equal volume fraction for investigations of the structural effects in the nano-materials. It is found that the strength of the nano-layered composites increases with decreasing thickness of the individual layer. The choice of material systems may influence the peak strength of the composites. Cold-rolled nano-multilayers show no dislocation cell formation upon a factor of two reduction in total multilayer thickness. To study fatigue, a novel experimental technique for performing high cycle and high stress bending fatigue experiment is introduced. Cu/Nb composite laminates with 40 nm individual layer thickness are tested and a fatigue S-N curve is obtained. Compared to bulk Cu, over an order of magnitude increase in the stress to failure is observed. The ratio of the fatigue endurance limit to the ultimate tensile strength is about 0.35. The nano-layered composites are potential candidates for applications such as hard coatings, x-ray optical elements microelectromechanical (MEMS) devices, and magnetic recording media.

1. Introduction

Research on mechanical properties of nano-structured materials has been conducted since the announcement of the potential benefits of nano-scale devices by Richard P. Feynman [1], or maybe earlier. Figure 1 schematically shows the current status of experimental results on single crystal (SC) and polycrystalline copper (Cu) with difference crystalline sizes. Single crystalline copper with naturally occurring dislocations inside exhibit lowest strength due to a defect-dominating deformation mechanism by dislocations [2, 3]. Conventionally metallurgical polycrystalline Cu exhibits higher strength with smaller grain sizes, due to the Hall-Petch type dislocation-based mechanisms. Materials consisting of nano-scale microstructures exhibit unusual mechanical properties, and hence are of scientific and industrial interest for further exploration. It has been shown that nano-layered multilayers exhibit ultra-high yield strength [4]. Transmission electron microscopy (TEM) studies on cold-rolled Cu/Nb multi-layers have shown that the films demonstrate large plastic deformation without the formation of dislocation cell structures [5].

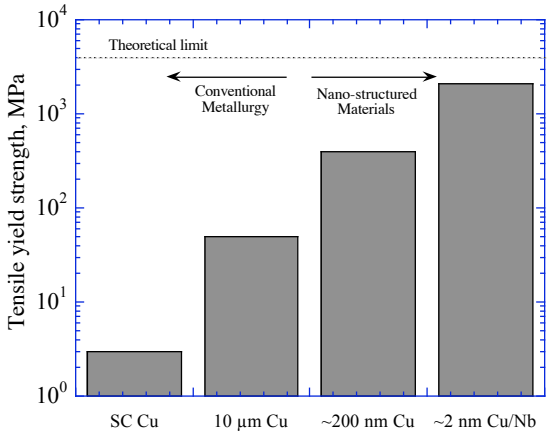

Figure 1. A schematic diagram to delineate the high tensile yield strength of nano-scale composites. Single crystal copper, denoted as SC Cu, shows lowest strength due to dislocations. Polycrystalline Cu with grain sizes of 10 µm and 200 nm shows a large increase in strength, due to the Hall-Petch effect. Cu/Nb multilayers with individual layer thickness of 2 nm exhibit the highest strength, approaching the theoretical limit calculated by E/30, where E is the Young's modulus of copper.

The mechanisms for high strength in the nano-layered composites can be understood as follows. According to molecular dynamics simulations, the origin of the peak strength of Cu/Nb multilayers having a layer thickness of around 2 - 4 nm can be understood in terms of the high interface barrier to single dislocation transmission [6]. The confined layer slip model of a single dislocation successfully explains the increase in strength with decreasing layer thickness at relatively higher layer thickness of around 5-100 nm, For layer thickness greater than 100 nm, the dislocation pile-up model, based on the Hall-Petch relationship, is applicable [7]. Recent experimental work on the

mechanical fatigue properties of the self-supported, nano-layered Cu/Nb composites show a dramatic increase in their fatigue endurance limit [8].

In the literature, fatigue studies on polycrystalline copper foils with micrometer-seze grains, tested *via* a flex fatigue method [9, 10] show that the transition from the plastic (low cycle) to elastic (high cycle) cyclic response occurs at about 10^4 cycles, and fatigue cracks initiate on the sample surface, and propagate along the grain boundaries across the sample width and through its thickness. Moreover, no cells or walls of dislocations can be found in the fatigued Cu foils, suggesting the dislocations move individually or in small groups and escape at the specimen surface. Also, dislocation activity associated with the plastic strain traverses the specimen in a direction at about 45° angle to both the load axis and through-thickness direction. Low cycle fatigue properties of copper foils with 25 μm thickness and about 1 μm grain sizes through tensile testing is studied in [11], and no dislocation cell structures with grain size smaller 2 μm are found. A high frequency (up to several kHz) tensile testing technique [12] is used to study annealed Cu foils, and it is found that the fatigue limit at 10^6 cycles is around 40 ~ 60 MPa, depending on foil thickness. Crack initiation sites are at the extrusions along the persistent slip bands (PSB's). Furthermore, fatigue results are identical in the range of testing frequency from 70 to 700 Hz. Upon load cycling, the initially equiaxed cellular microstructure of their specimens becomes elongated one, and then transforms into persistent slip bands.

For fatigue properties of nanocrystalline Cu, literature is limited. Zhang *et al*. [13] perform TEM studies on tensile fatigued thin copper films with 200 nm thickness, and found less fatigue damage, such as extrusions and dislocation cell structures, due to the prevention of localized accumulation of plastic strain within grains through reduction of grain size. It is speculated [13] that the nano-scale film thickness promotes the formation of damage such as cracks at twin and grain boundaries during fatigue. Therefore, conventional fatigue mechanisms cannot be applied to nano-materials. Tension-tension fatigue properties of nanocrystalline (nc) copper show that the nc Cu is more robust against fatigue damage than the conventional bulk Cu [14]. The damage mechanism is identified to be associated with the formation of the persistent slip bands (PSB's) and parallel micro-meter size extrusions are observable on the surface. In both of the above studies, quantitative fatigue results in terms of S-N curves (S refers to the maximum stress and N to the number of cycles to failure) are not available. As for multilayered nano-materials, Stoudt *et al*. [15, 16] investigate the influence of multilayered Cu/Ni coatings on Cu substrate for their fatigue properties, and revealed a significant improvement in the fatigue crack initiation. They demonstrate that a judiciously chosen coating may largely increase the fatigue life of the coated materials.

As for the fatigue testing methods, conventional methods such as the tension-tension and rotating-beam fatigue testing method, well documented in many textbooks [17, 18], have several drawbacks when applied to self-supported thin films. The main one is the quality of alignment due to the smallness of specimens. Vibrating cantilever techniques have been used by Connally and Brown [19] to study slow crack growth in single-crystal silicon, and by van Aredell and Brown [20] on crack growth in silicon

MEMS devices. Moreover, Schwaiger and Kraft [21] have performed high cycle fatigue testing on silver films on the SiO_2 substrate in the form of cantilever microbeams deformed by a nano-indenter through the continuous stiffness measurement method. The resonant fatigue method (discussed in Section 2.5) is superior to traditional methods in that high stress and high cycle fatigue can be accomplished simultaneously with fewer alignment problems. This method applies fully reversed stress to specimens, i.e. the load ratio $\sigma_{min}/\sigma_{max} = -1$.

Renewed interest in experimentally studying the vibrational dynamics of cantilever beams in mechanics has arisen from advances in microelectromechanical systems (MEMS), nanoelectromechanical systems (NEMS) and nanoscale material property measurement. Novel experimental methods, such as atomic force microscopy (AFM) [22], and development of high frequency mechanical resonators [23] also spur this research field. The work by Tilmans [24] provides a comprehensive resource on mechanical resonators. Research on mechanical properties of materials via cantilever beams are numerous. For example, Yang *et al.* [25] characterizes the energy dissipation properties of single-crystal silicon and Chen *et al.* [26] studies the properties of quartz microfibers. Study of carbon nano tubes through vibrating cantilever beams has been reported in [27]. Further review on microscale mechanical testing methods, in general, can be found in [28].

2. Experiment

This section is organized as follows. First, the sample preparation is presented, followed by the discussion of thermal, morphological stability of the nano-layered composites. Then, tensile and hardness properties of the nano-multilayers are presented. Finally, the resonant fatigue device and its results are discussed.

2.1 Plasma sputtered thin films

With the maturity of sputtering deposition techniques, thin films consisting of individual layers with thickness of a few nanometers up to a few microns can routinely be prepared. For the fatigue study with the resonant fatigue device (discussed in Section 2.5), Cu/Nb multilayers, with individual layer thickness of 40 nm and consisting of 500 bilayers of Cu and Nb with a total multilayer thickness of 40 μm, are prepared by magnetron sputtering deposition on silicon wafers. Magnetron sputtering deposition parameters are so chosen that residual stresses in the films are slightly compressive [29]. After deposition, the samples are peeled off from the substrates. Following a pre-cut pattern of the substrate, our sample dimensions are 2 mm long, 1 (or 0.5) mm wide and 40 μm thick. A typical cross-sectional TEM image of the Cu/Nb multi-layers is shown in Figure 2 along with selected area diffraction pattern. Note the polycrystalline structure of the layer with in-plane columnar grain size on the order of the layer thickness. The multilayers exhibit a strong Kurdjumov-Sachs orientation relationship: {111}Cu // {110} Nb, and <110>Cu // <111>Nb. The parallel {111}Cu and{110} Nb planes form the interface.

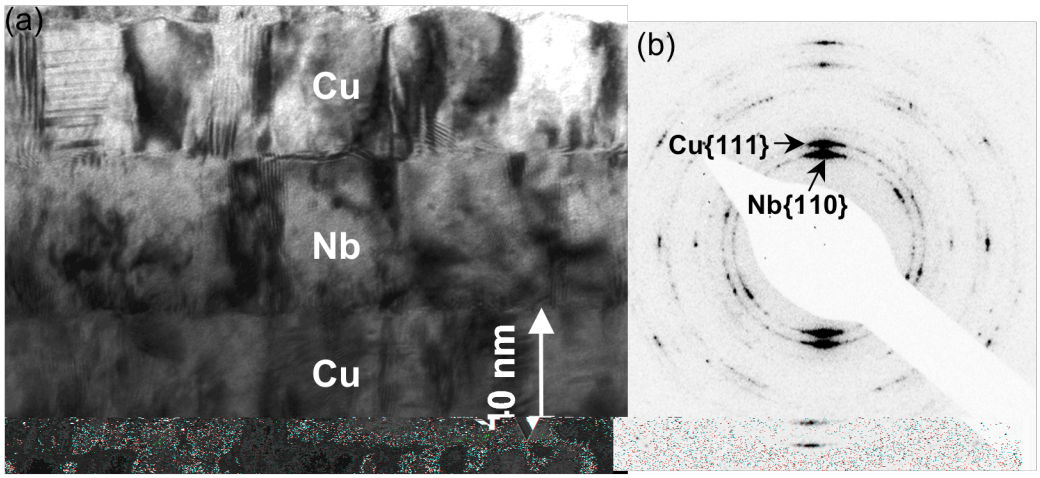

Figure 2. (a) Transmission-electron microscopic (TEM) image of the Cu/Nb multilayer with alternating, 40-nm thick (each) copper and niobium layers. Columnar grains in each layer are observable. (b) Selected area electron diffraction image showing the texture of the Cu and Nb layers. The Kurdjumov-Sachs orientation, i.e. {111}<110> Cu and {110}<111> Nb, is at the interface between the two crystals [8].

2.2 Thermal, morphological stability

The thermal stability is crucial in exploiting the novel structural and functional properties of nanoscale multilayered materials for advanced engineering applications. Conventional experiment for thermal stability testing is to expose samples at elevated temperature or thermal cycling, and to monitor the morphological structure of the sample after cooling. For example, W/NbN multilayers in the single-crystal form with low-energy coherent interfaces have excellent thermal stability at elevated temperatures [30]. The elastic stress-driven instability mechanisms in single crystal multilayers are theoretically analyzed in [31]. Morphological evolution in nanoscale multilayers such as Cu/Nb where the constituent layers do not form intermetallic compounds and have insignificant mutual solid solubility, and no phase transformation within each layer (e.g. amorphous to crystalline) with increasing temperature is possible. From the annealing experiments on the 75 nm Cu/Nb multilayers up to 800˚C for an hour [32], it is found that (1) the layer structure is maintained, i.e. no significant geometric rearrangement of the layered structure, (2) there is no measurable change in the individual layer thickness, and (3) the in-plane grain size increases. In other words, the nano-scale Cu/Nb multilayers are morphological stability under heat treatment up to 800˚C.

2.3 Tensile test

Although tensile testing has long been a standard practice in determining the mechanical properties of materials, conventional tensile testers pose severe danger to ultra-thin specimens. Tensile machines with hydraulic servomechanism for feedback may easily introduce noise displacement vibration on the order of tens of microns, which may be comparable to the specimen size or thickness. A genuine solution is to use a micro tensile tester, as described in [33], and results show that the 75 nm Cu/Nb foils maintain

layered structure until fracture at an elevated temperature. With caution and a double-sample design using a dummy annealed Cu specimen, Figure 3 shows the tensile test results of the 100 nm Cu/Nb multilayer in terms of true stress and true strain. It can be seen that the ultimate tensile stress is about 1.3 GPa, and with the 0.2% rule the yield stress can be determined to be 850 MPa. The measured Young's modulus is about 110 GPa, and a significant amount of plastic strain is observed.

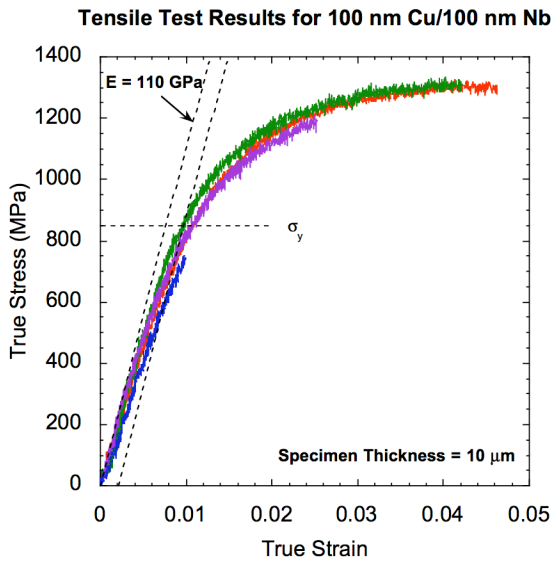

Figure 3. Tensile test results of the 100 nm Cu/Nb multilayer (courtesy of J. G. Swadener). Ultimate tensile strength is about 1.3 GPa, and yield strength 850 GPa from the 0.2% rule. Young's modulus is determined about 110 GPa. Total multilayer thickness is 10 μm.

2.4 Hardness test

Investigation of the surface hardness utilizes an indentation load-depth sensing apparatus, the so-called nanoindenter. It directly measures the load on a diamond Berkovich indenter tip as a function of displacement from the surface. Hardness is determined from the ratio of load to the projected area of the indent. The area function is determined by an iterative process involving indents into materials of known isotropic properties (e.g. fused quartz). Following the Oliver and Pharr method [34], the unloading portion of the curve is used to estimate the elastic modulus of the specimen. Figure 4 shows a typical, repeated nanoindentation test on Cu/Nb multilayers, and the measured hardness and Young's modulus are about 6 GPa and 115 GPa [7], respectively, within experimental errors.

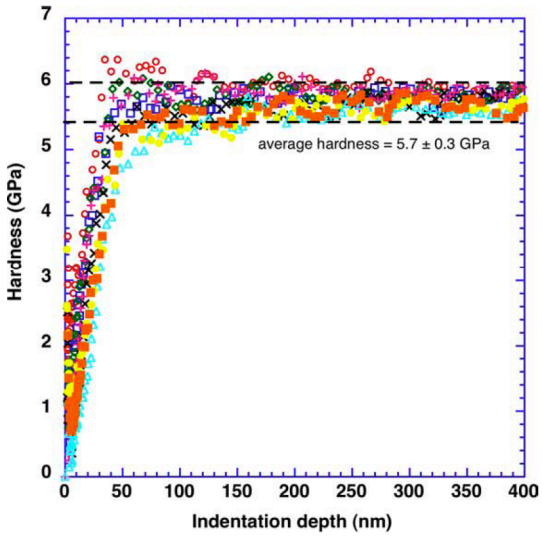

Figure 4. Nanoindentation hardness vs. depth for 5 nm Cu/Nb multilayers on substrate [7], tested with the continuous stiffness method. The measured hardness is about 5.7 GPa, and Young's modulus from the unloading slope is about 115 GPa. The hardness measures below 50 nm indentation deep are unreliable due to the limitation of the tip area function calibration.

2.5 Resonant fatigue test

The resonant fatigue device [35] is designed to measure fatigue properties of the nano-layered Cu/Nb foils in terms of the S-N curves, where S refers to the maximum tensile stress during fully reversed tension-compression cyclic loading and N to the number of cycles to failure. The schematic of the experimental setup is shown in Figure 5. A bimorph piezoelectric plate-like actuator is used to generate excitation at the support of a cantilever beam specimen. The bimorph actuator is clamped into the foundation with properly electrical connections, and driven by a signal function generator. The displacements of the specimen and aluminum clamp are monitored by a fiber-optic measurement system with the probes labeled Fiber 1 and Fiber 2, respectively. The displacement difference between the two probes gives rise to actual deformation of the cantilever specimen. The fatigue failure is defined to be the near initiation of a macro crack. In practice, a 10-Hz algorithm is adopted, that states a sample fails when a 10 Hz reduction in its resonant frequency is observed. Remark that due to the lack of a clearly defined gage section, cracks with very small lengths cannot be detected with our method. The 10-Hz algorithm would determine a crack only above a certain length, and it is reasonable to consider this failure definition to be close to the one that determines the initiation of a crack.

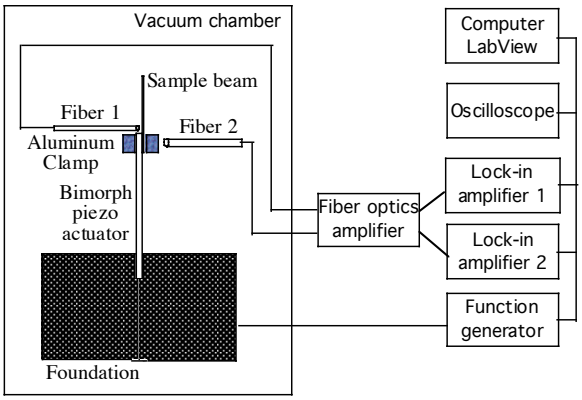

Figure 5. Schematic of the resonant fatigue device. A bimorph piezo actuator is clamped into the properly electrically connected foundation, and a cantilever specimen is mounted at the top of the piezo. Displacements are monitored through fiber-optic probes [35].

Figure 6 shows a typical frequency scan result of the specimen from the resonant frequency device. The resonant frequency can be determined by identifying the peak of normalized displacement difference or the phase shift at 90˚. The normalized displacement difference is defined as the ratio of the difference of the displacements of the Cu/Nb specimen and the tip of the piezo actuator to the displacement of the piezo. Unlike the usual frequency response of a one degree-of-freedom harmonic oscillator, beyond the resonance, the system demonstrates negative displacement difference and drop of the phase shift back to -180˚. For this specific case in Figure 6, the resonant frequency is about 337 Hz. Remark that the clamped boundary condition can be monitored for sliding by performing the frequency scan, especially after a long run fatigue experiment. No changes in resonant frequency indicate no changes in both the mechanical assembly of the setup and the material properties of the specimen. Based on the texture of the sample (<111> for Cu and <110> for Nb pointing to the direction perpendicular to the surface) and C_{ijkl} found in the literature, the in-plane Young's modulus can be theoretically calculated to be about 115 GPa for the Cu/Nb composite with the equal volume fraction of Cu and Nb through a uniform homogenization procedure [36].

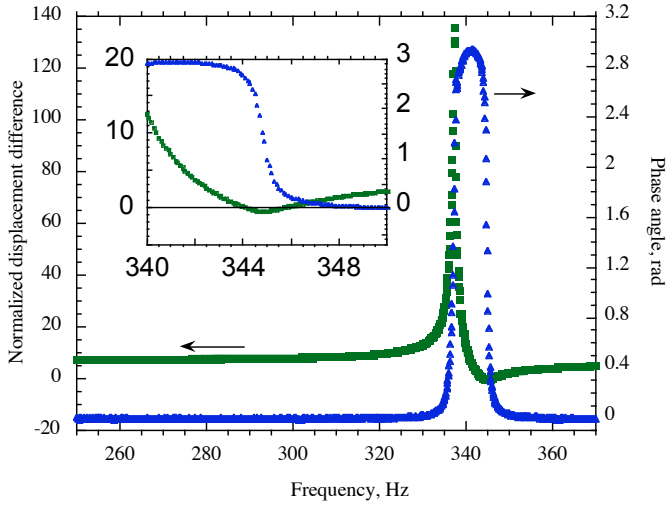

Figure 6. A typical frequency scan result of the resonant fatigue device. Resonance is at about 337 Hz, and an anti-resonant peak is present at 345 Hz. Phase change is not quite 180° due to effects of damping. Young's modulus of the specimen can be readily calculated from the measured resonant frequency [35].

A typical SEM picture of the fatigue crack observed on the Cu/Nb multilayers before complete fracture is shown in Figure 7 (a). The length of the sample was 7.1 mm, and the crack caused an about 60 Hz reduction in resonant frequency. This sample was cycled at the stress amplitude 800 MPa for 8500 cycles. The position of the crack is very near the aluminum clamp. The bright spots are the cyanoacrylate glue used to pre-mount the specimen on the piezo actuator before mounting the aluminum clamp and fatigue testing. Fatigue damage such as extrusions and intrusions are not observed around the crack on the surface where maximum stress was exerted. In contrast, Figure 7 (b) and (c) show typical SEM pictures of the fatigue damage done by the resonant fatigue device on annealed Cu specimens. Classical fatigue damage is present. It is conceivable that cracks were initiated from the edge of the specimen (maybe due to some stress concentrator), and then propagated both across the width and through the thickness of the specimen. Along the cracks, persistent slip bands are visible.

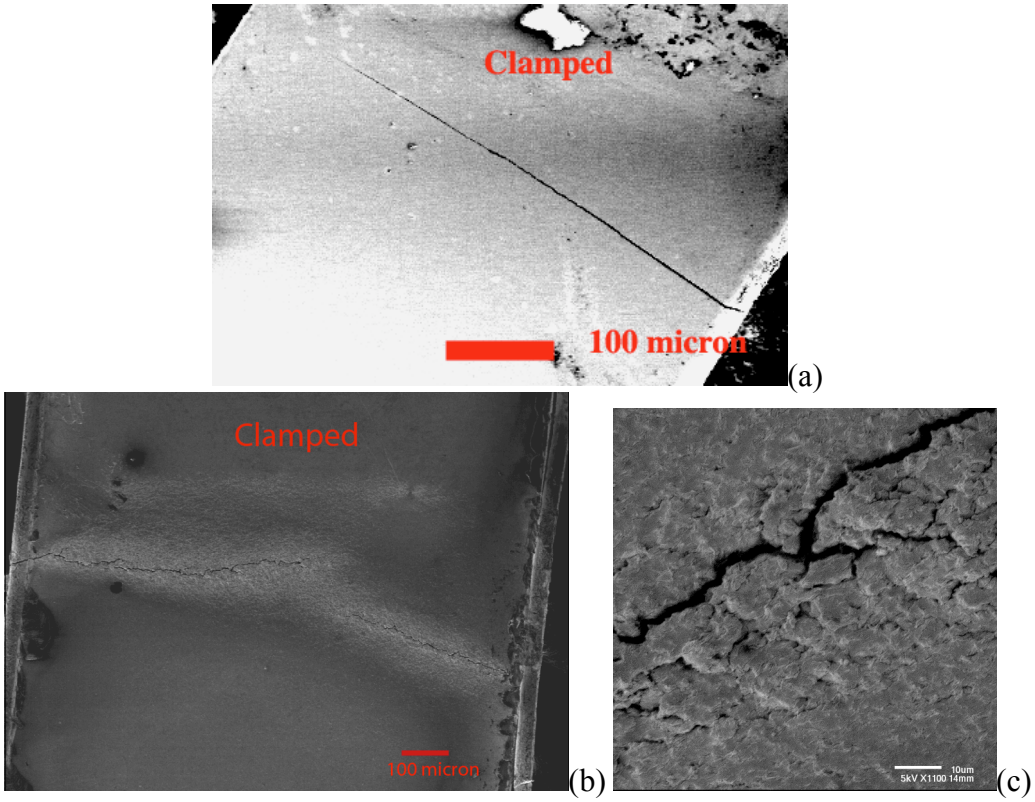

Figure 7. (a) SEM image of the fatigued Cu/Nb nano-multilayer [8]. No persistent slip bands are observable. (b) SEM image of the fatigued annealed Cu. Clear fatigue damage is present. (c) High-magnification SEM image of a crack in (b), showing the fatigue crack marches along persistent slip bands.

Figure 8 (a) shows the S-N curve of the 40 nm Cu/Nb multilayer, along with annealed Cu, Al6061 alloy, low carbon steel and high strength steel, for comparison. Fatigue endurance limit of the materials is normalized with respect to the ultimate tensile strength in Figure 8 (b). The nano-layered Cu/Nb exhibits a fatigue limit at about 450 MPa with a normalized fatigue limit of 0.35. It can be seen that the high fatigue endurance of the 40 nm Cu/Nb multilayers correlates well with its high tensile strength of around 1400 MPa. The deformation mechanism of the fatigue of the 40 nm Cu/Nb multilayers is not completely understood. Since the formation of dislocation cell structures is not present due to the nanoscale thickness of an individual layer between two adjacent interfaces, extrusion or intrusion is not observed on the surface subjected to maximum stress. This is consistent with our experimental findings. However, concerning detailed deformation mechanisms, specifically how the nano-layered thin films accumulate damage during cycling loading that eventually leads to fatigue crack initiation require further experimental and theoretical study.

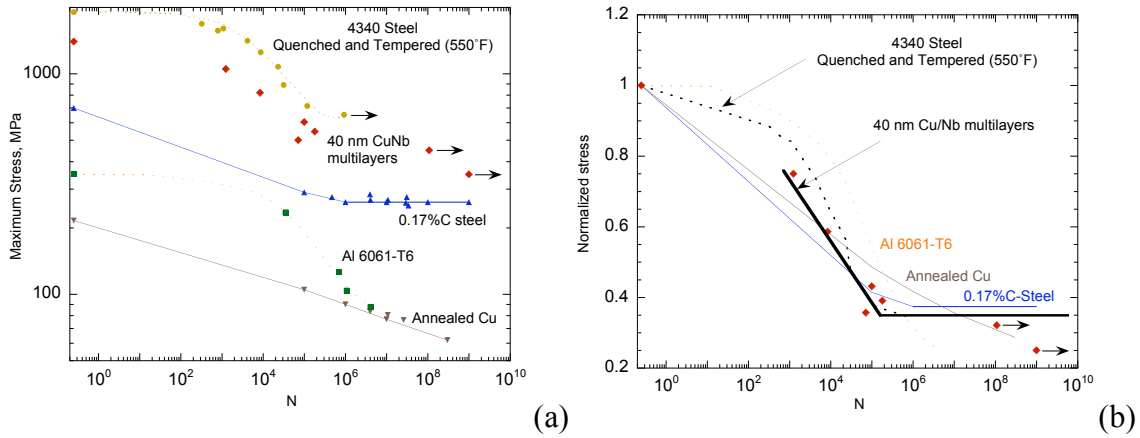

Figure 8. (a) Fatigue S-N curves of annealed Cu, Al 6061-T6 alloy, low carbon steel, 40 nm Cu/Nb, and high strength steel. Except for the Cu/Nb multilayer, data for other materials are taken from the literature. The 40 nm Cu/Nb shows a fatigue endurance limit of 450 MPa. (b) Normalized fatigue S-N curves with respect to the ultimate tensile strength. The Cu/Nb multilayers exhibits a normalized fatigue limit of 1/3, similar to materials in the bulk form.

3. Theory

Theoretical work in predicting or modeling the behavior of nano-layered composites can be performed *via* dislocation models in the frame work of elasticity or molecular dynamics simulations. Continuum viscoplastic composite models may also provide significant inside into the deformation mechanisms of the nano-multilayers [37].

3.1 Hall-Petch relationship

Figure 9 shows the strength of Cu/Nb multilayers plotted as inverse square-root of the layer thickness.. A linear fit to the data at the coarsest length scales is consistent with the Hall–Petch model. For layered structures, the variable h indicates the thickness of an individual layer.

$$\sigma_y = \sigma_0 + k_y h^{-n} \qquad (1)$$

Here σ_y is the yield strength, k_y is the Hall–Petch slope and σ_0 is a measure of the lattice friction stress to slip. The Hall-Petch relationship dictates n = 0.5. Experimental yield stress can be obtained from the empirical relationship H = 2.7 σ_y. Remark, in addition to dislocation pile-ups, other mechanisms such as emission of dislocations from grain boundary ledges have been used to derive Eq. (1) for equi-axed grain single-phase materials [38]. For multilayered structures, misfit dislocations at the interface would typically have a Burgers vector component in the interface plane, and the ledges that would emit dislocations across the interfaces may not be readily available, so the pile-up

model is more appropriate. From Figure 9, σ_0 can be estimated to be about 700 MPa, and $k_y \sim 0.2$ MPa$\sqrt{m}$, which correlate well with peak strength [7].

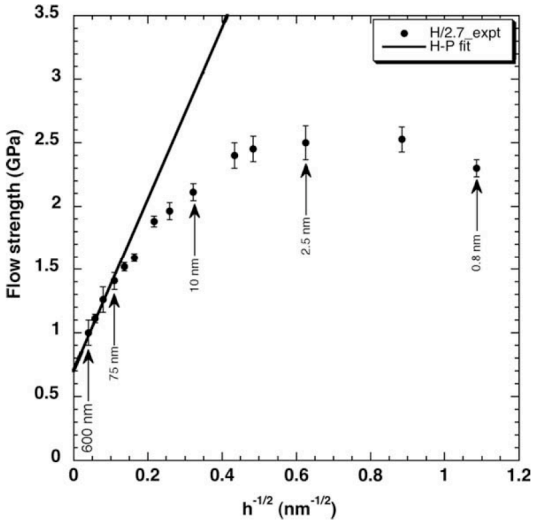

Figure 9. Hall-Petch plot of Cu/Nb multilayers [7]. Data points are calculated from hardness divided by 2.7, and the linear curve fit indicates the prediction of Hall-Petch (H-P) relationship. The breakdown of the H-P is due to the failure of dislocation pile-up model at smaller individual layer thicknesses.

3.2 Breakdown of Hall-Petch relationship

The breakdown of Hall-Petch behavior (i.e. deviation from linearity) in nanoscale materials implies that the deformation is no longer controlled by dislocation pile-ups. Discrete pile-ups may provide mechanisms for non-Hall-Petch behavior; elasticity-based calculations have predicted that, for single ended dislocation pile-ups, $H \propto h^{-0.5}$ is only applicable when the number N of dislocations in a pile-up is more than six [39]. Orowan loop-type arguments, Eq. (2), to describe confined layer slips, may lead to a different relationship between peak strength and layer thickness. A schematic diagram to delineate the motion of dislocations being confined in individual layers, as shown in Figure 10 [40].

$$\sigma_y \propto \frac{\ln(h/b)}{h} \tag{2}$$

Here b indicates the Burgers vector. According to current understanding of the strengthening mechanisms of nano-multilayers, the evolution of their strength as a function of layer thickness may be divided into four regimes in terms of individual layer thickness [41].

a) *Layer thickness of 10 ~ 100 nm*: The Hall-Petch relationship stands, $\sigma \propto h^{-1/2}$.
b) *Layer thickness of 5 ~ 10 nm*: Strength increases with reduction of layer thickness, $\sigma \propto h^{-n}$, where $n \neq 0.5$.

c) *Layer thickness of 2 ~ 5 nm*: A strength peak is present during the transition from step b) to step c).
d) *Layer thickness of 1 ~ 2 nm*: Strength decreases with decreasing layer thickness.

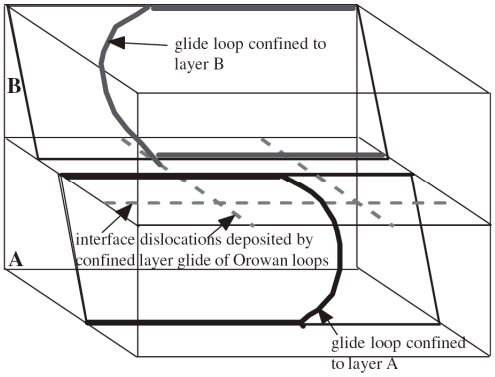

Figure 10. The dislocation mechanism of confined layer slips [40]. When individual layer thickness is small enough, limited room prevents dislocation pile-ups. With certain interfacial strength, dislocations may be confined to move in a single layer, causing strength increases not followed by the Hall-Petch relationship.

3.3 Molecular dynamics simulations

The great benefits from molecular dynamics (MD) simulations of the multilayer systems are detailed considerations of the dislocation core structure and interfacial coherency [6, 42]. It is found that certain core structures of misfit dislocations may effectively remove local coherency stress, promote dislocation mobility, and lead to weak interfaces. Since intrinsic resistance to slip transmission originates from the low shear strength of the interfaces, the stress field of a glide dislocation approaching the interface can locally shear a weak interface leading to dislocation absorption and core spreading along the interface. Therefore, weak interfaces give rise to high strength of nano-multilayers. It is calculated that extremely high applied stress, on the order of a few GPa at 0 K simulation environment, may be needed to activate dislocations along the interface. Thermal activation at 300 K may reduce the predicted strength to a level that is comparable to the 2.5 GPa peak strength inferred from nano-indentation experiments.

4. Summaries

From experiment, continuum theory and molecular dynamics simulations, nano-scale metallic multilayers have been examined to show high yield and tensile strengths, thermal stability, ductility and high fatigue endurance. The resonant fatigue device is efficient for fatigue testing of self-supported thin-film materials. Cu/Nb multilayers with 40 nm individual layer thickness exhibit a fatigue endurance limit of 450 MPa. The ratio of the fatigue endurance limit to ultimate tensile strength is found to be around 0.35, consistent with similar empirical scaling observed in other materials in the bulk form, which may indicate a defect-control fatigue mechanism. With even smaller individual

layer thickness, it is hypothesized that the fatigue endurance limit might approach the yield strength of the multilayers.

5. Acknowledgements
The author wishes to acknowledge the collaboration with Drs J. G. Swadener, A. Misra, R. G. Hoagland, M. Nastasi, J. P. Hirth, N. Mara, and M. Demkowicz at Los Alamos National Laboratory, where research on nano-layered composites is most actively being currently pursued, while he was a postdoctoral fellow there. Great environment for teaching and research in the Department of Civil Engineering at National Cheng Kung University is also gratefully appreciated.

References

[1] R. P. Feynman. There's plenty of room at the bottom. *Engineering and Science*, 23:22–36, 1960.
[2] J. P. Hirth and J. Lothe. *Theory of dislocations*. John Wiley & Sons, Inc., New York, NY, 1982.
[3] D. Hull and D. J. Bacon. *Introduction to dislocations, 4th Edition*. Butterworth Heinemann, Oxford, 2001.
[4] B. M. Clemens, H. Kung, and S. A. Barnett. Structure and strength of multilayers. *MRS Bulletin*, 24(2):20–26, 1999.
[5] A. Misra, X. Zhang, D. Hammon, and R. Hoagland. Work hardening in rolled nanolayered metallic composites. *Acta Materialia*, 53:221–226, 2005.
[6] R. Hoagland, R. Kurtz, and C. Henager. Slip resistance of interfaces and the strength of metallic multilayer composites. *Scripta Materialia*, 50(6):775–779, 2004.
[7] A. Misra, J. Hirth, and R. Hoagland. Length-scale-dependent deformation mechanisms in incoherent metallic multilayered composites. *Acta Materialia*, 53:4817–4824, 2005.
[8] Y. C. Wang, A. Misra, and R. G. Hoagland. Fatigue properties of nanoscale Cu/Nb multilayers. *Scripta Materialia*, 54:1593–1598, 2006.
[9] H. Merchant, M. Minor, and Y. Liu. Mechanical fatigue of thin copper foil. *Journal of Electronic Materials*, 28(9):998–1007, 1999.
[10] D. Read. Tension-tension fatigue of copper thin films. *International Journal of Fatigue*, 20(3):203–209, 1998.
[11] S. Hong and R. Weil. Low cycle fatigue of thin copper foils. *Thin Solid Films*, 283:175–181, 1996.
[12] M. Judelewicz, H. Kunzi, N. Merk, and B. Ilschner. Microstructural development during fatigue of copper foils 20-100 mm thick. *Materials Science and Engineering A*, 186:135–142, 1994.
[13] G. Zhang, C. Volkert, R. Schwaiger, E. Arzt, and O. Kraft. Damage behavior of 200-nm thin copper films under cyclic loading. *Journal of Materials Research*, 20(1):201–205, 2005.
[14] A. Witney, P. Sanders, J. Weertman, and J. Eastman. Fatigue of nanocrystalline copper. *Scripta Metallurgica et Materialia*, 33(12):2025–2030, 1995.
[15] M. R. Stoudt, R. C. Cammarata, and R. E. Ricker. Suppression of fatigue cracking with nanometer-scale multilayered coatings. *Scripta Materialia*, 43:491–496, 2000.

[16] M. R. Stoudt, R. E. Ricker, and R. C. Cammarata. The influence of a multilayered metallic coating on fatigue crack nucleation. *International Journal of Fatigue*, 23:S215–S223, 2001.
[17] N. Frost, K. I. Marsh, and L. P. Pook. *Metal Fatigue*. Clarendon Press, Oxford, UK, 1974.
[18] S. Suresh. *Fatigue of Materials*. Cambridge University Press, Cambridge, UK., 1998.
[19] J. A. Connally and S. B. Brown. Slow crack growth in single-crystal silicon. *Science*, 256:1537–1539, 1992.
[20] W. W. van Aesdell and S. B. Brown. Subcritical crack growth in silicon MEMS. *IEEE Journal of Microelectromechanical Systems*, 8(3):319–327, 1999.
[21] R. Schwaiger and O. Kraft. High cycle fatigue of thin silver films investigated by dynamic microbeam deflection. *Scripta Materialia*, 41(8):823–829, 1999.
[22] G. Binnig, C. Quate, and C. Gerber. Atomic force microscope. *Physical Review Letters*, 56(9):930–933, 1986.
[23] X. M. H. Huang, C. A. Zorman, M. Mehregany, and M. L. Roukes. Nanodevice motion at microwave frequencies. *Nature*, 421:496, 2003.
[24] H. A. C. Tilmans, M. Elwenspoek, and J. H. J. Fluitman. Micro resonant force gauges. *Sensors and Actuators A*, 30:35–53, 1992.
[25] J. Yang, T. Ono, and M. Esashi. Energy dissipation in submicrometer thick single-crystal silicon cantilevers. *Journal of Microelectromechanical Systems*, 11(6):775–783, 2002.
[26] X. Chen, S. Zhang, G. J. Wagner, W. Ding, and R. S. Ruoff. Mechanical resonance of quartz microfibers and boundary condition effects. *Journal of Applied Physics*, 95(9):7823–4828, 2004
[27] M. F. Yu, M. J. Dyer, J. Chen, and K. Bray. Multiprobe nanomanipulation and functional assembly of nanomaterials inside a scanning electron microscope. In *Int. Conf. IEEE-NANO2001*, Maui, 2001.
[28] V. T. Srikar and S. M. Spearing. A critical review of microscale mechanical testing methods used in the design of microelectromechanical systems. *Experimental Mechanics*, 43(3):238–247, 2003.
[29] X. Zhang and A. Misra. Residual stresses in sputter-deposited copper/330 stainless steel multilayers. *Journal of Applied Physics*, 96(12):7173–7178, 2004.
[30] S. A. Barnett, A. Madan, I. Kim, and K. Martin. Hardness and stability of metal–nitride nanoscale multilayers. *Scripta Materialia*, 50(6):739–744, 2003.
[31] N. Sridhar, J. M. Rickman, and D. J. Srolovitz. Multilayer film stability. *Journal of Applied Physics*, 82(10):4852–4859, 1997
[32] A. Misra, R. G. Hoagland, and H. Kung. Thermal stability of self-supported nanolayered Cu/Nb films. *Philosophical Magazine*, 84(10):1021–1028, 2004.
[33] N. Mara, A. Sergueeva, A. Misra, and A. K. Mukherjee. Structure and high-temperature mechanical behavior relationship in nano-scaled multilayered materials. *Scripta Materialia*, 50:803–806, 2004.
[34] W. C. Oliver and G. M. Pharr. An improved technique for determining hardness and elastic modulus using load and displacement sensing indentation experiments. *Journal of Materials Research*, 7(6):1564–1583, 1992.
[35] Y. C. Wang, T. Hoechbauer, J. G. Swadener, A. Misra, R. G. Hoagland, and M. Nastasi. Mechanical fatigue measurement via a vibrating cantilever beam for self-supported thin solid films. *Experimental Mechanics*, 46:503–517, 2006.

[36] A. E. H. Love. *A treatise on the mathematical theory of elasticity*. Dover Publications, New York, NY, 1944.

[37] K. Al-Fadhalah, C. N. Tome, A. J. Beaudoin, I. M. Robertson, J. P. Hirth, and A. Misra. Modeling texture evolution during rolling of a Cu–Nb multilayered system. *Philosophical Magazine*, 85(13):1419–1440, 2005.

[38] H. H. Fu, D. J. Benson, and M. A. Meyers. Homogenization method for strength and inelastic behavior of nanocrystalline materials. *International Journal of Plasticity*, 21(1):67–82, 2005.

[39] H. Liu and Q. Gao. The equivalence between dislocation pile-ups and cracks. *Theoretical and Applied Fracture Mechanics*, 12(3):195–204, 1990.

[40] A. Misra and H. Kung. Deformation behavior of nanostructured metallic multilayers. *Advanced Engineering Materials*, 3(4):217–222, 2001.

[41] A. Misra, J. P. Hirth, and H. Kung. Single-dislocation-based strengthening mechanisms in nano-scale metallic multilayers. *Philosophical Magazine A*, 82(16):2935–2951, 2002.

[42] R. G. Hoagland, T. E. Mitchell, J. P. Hirth, and H. Kung. On the strengthening effects of interfaces in multilayer fcc metallic composites. *Philosophical Magazine A*, 82(4):643–664, 2002.